Journal of Optoelectronics and Advanced Materials Vol. 7, No. 5, October 2005, p. 2317 - 2322

PHOTOCURRENT RELAXATION IN As_xSe_{1-x} THIN FILMS: COMPOSITIONAL DEPENDENCE

M. S. Iovu, I. A. Vasiliev*, D. V. Harea, E. P. Colomeico

Centre of Optoelectronics, 1 Academiei str., MD-2028, Chisinau, Moldova Republic

Photocurrent relaxation technique has been used to study the deep states in amorphous arsenic-selenium films As_xSe_{1-x} with x=0.02, 0.05, 0.1, 0.28, 0.4, 0.45, 0.5 and 0.6 using monochromatic light pulse (λ=0.63 μm, $\Phi=(1\text{-}3)\cdot 10^{14}$ (photon) $cm^{-2}s^{-1}$, τ~25 s) at room temperature. The i_{ph} x t vs. kTln(νt) diagrams are used to evaluate the density-of-state (DOS) distribution in analogy with time-of-flight (TOF) post-transit photocurrent analysis. For the composition of x=0.02 this distribution consist of a broad maximum located near 0.69 eV. As the concentration of arsenic increase the position of the maximum increase up to 0.84 eV at x=0.4 and it width also increase in this range of composition. On contrary, for x>0.4 the DOS function consist of the narrow peak extended in the mid-gap and it intensity abrupt falls for x=0.45 and 0.5. By comparison with the steady-state photocurrent spectra the relaxation of photocurrent for x<0.4 have been interpreted as due to deep acceptor-like centers associated with D^+ and D^- defects with negative U^-. For x>0.4 such interpretations suggest the reductions in defect densities because stressed rigid phase.

(Received May 20, 2005; accepted September 22, 2005)

Keywords: Photocurrent relaxation, amorphous arsenic-selenium films, defect centers

1. Introduction

Arsenic selenide glasses are widely studied materials because of their unique light-induced effects. Recently new effects in the As-Se binary system such as photo-darkening, photo-crystallization, photo-melting and photo-expansion have been observed. They have stimulated new applications of these non-oxide glass materials in modern optoelectronics [1-6].

The new insight into the origin of these effects becomes from the elastic properties of glassy network in floppy, intermediate and stressed rigid phases [7]. For example, it was demonstrated, that opto-mechanical effects observed in As_xSe_{1-x} thin films are more pronounced in As-rich compositions near x = 0.5 and 0.57 than at the stoichiometric composition with x=0.4 because stressed rigid phase. The experimental evidence for this rigid percolation transition comes from T-modulated differential scanning colorimetry and Raman scattering, but little knowledge of the electronic structure of arsenic selenide thin films has been accumulated.

Photocurrent relaxation technique (PRT) is a powerful tool to investigate the amorphous materials and it is used to probe the density of deep states distributed in mobility gap [8]. In addition, the deep states in glassy As_xSe_{1-x} can be associated with under-coordinated (states near the top of valence band) and over-coordinated (states near the bottom of conduction band) chalcogen atoms and it is obviously, that their density decrease when content of arsenic atoms in film is increased [9].

In this paper we examine the amorphous As_xSe_{1-x} films with different concentrations of arsenic atoms using PRT. The steady-state photocurrent spectra measurements also have been performed to investigate the density of states distribution in these samples.

* Corresponding author: ivasilev@phys.asm.md

2. Experimental

The PRT setup employs a monochromatic light sources (λ=0.63 μm, Φ=(1-3)$\times 10^{14}$ (photon) $cm^{-2}s^{-1}$), electromechanical shutter, an electrometer and X-Y recorder. The shutter is gated using pulse of waveform generator. The relaxation of the photocurrent curves where recorded over the large time scale from 0.1 up to 150 s at room temperature. The a-As_xSe_{1-x} films have been obtained from bulk As_xSe_{1-x} glass with different As content (x=0.02, 0.05, 0.1, 0.28, 0.4, 0.45, 0.5, 0.6) by the thermal evaporation in vacuum; the films (thickness L~2 μm) were sandwiched between aluminums electrodes (S~0.56 cm^2) one of witch was semitransparent.

The steady-state photocurrent spectrum was determined by measuring photocurrent signal as a function of photon energy in the range from 0.8 up to 1.8 eV. Other experimental details are available elsewhere [10,11].

3. Theoretical background

PRT measures photocurrent after cessations illumination, i.e. relaxation of photoconductivity. On the large time scale t the photocurrent i_{ph} decays due to capture of non-equilibrium charge carriers (holes) by tail state and deep acceptor-like centers distributed in energy and later on, due to recombination. The bimolecular recombination is typical for amorphous chalcogenide. If it is the case, the theory [12] gives an expression for time dependence of photocurrent:

$$i_{ph}(t) = e\left(\frac{\mu_c}{R}\right) FS\frac{kT}{t} g(E)\left[\int_E^{\infty} dE' g(E')\right]^{-1}, \tag{1}$$

where e is the elementary charge, μ_c – the free carrier mobility, R – the recombination coefficient, k – the Boltzman constant, T – the temperature, E - the energy, F-electric intensity and g(E) is the density of states distribution (DOS-function). Since the g(E) is predominantly determined by deep states, the PRT allows the study of defects in As_xSe_{1-x} films.

4. Experimental results

Fig. 1 shows the relaxation of photocurrent in amorphous As_xSe_{1-x} films after the long-time (about 25 s) monochromatic illumination. The decay of the photocurrent appears to be non-exponential. We can observe at least two distinct regions in the i_{ph} (t) curves: a fast process occurring immediately after switching off the illumination and a following long-term relaxation, i.e. persistent photocurrent, which increase for the samples with x>0.4 (Fig. 1b). The decay of the photocurrent after switching off the illumination may be approximated by a stretched-exponential function $i_{ph}(t)=i_{ph}(0)\exp[-(t/\tau)^{\alpha}]$+ const, where α is the dispersion parameter ($0<\alpha<1$), τ is the characteristic decay time constant, i_{ph} (0) is the steady-state photocurrent. A least-squares fit to the experimental data yields a decay exponent α~0.14 for the samples with x=0.4, which is comparable to previously reported values for As_2Se_3 amorphous films α=0.16 [13].

In Fig. 2, the experimental data of Fig. 1 are used to construct $I_{ph}(t)\times t$ versus $kT\ln(\nu t)$ diagrams in analogy with those that would represent the underlying DOS in the case of a TOF post-transit photocurrent analysis (PTPA). Differences are observed between the curves for non-stoichiometric As_xSe_{1-x}, but in data sets generated at different x exhibit the mutual agreement that they must have if they are to represent the DOS. An analysis in terms of Eqs. (1) becomes feasible if a superposition of an exponential band-tail and a Gaussian distribution of deep traps is used for g(E)

$$g(E) = \frac{N_t}{E_0}\exp\left(-\frac{E}{E_0}\right) + \frac{N_d}{\sqrt{2\pi}\sigma}\exp\left[-\frac{(E-E_d)^2}{2\sigma^2}\right], \tag{2}$$

with N_d and E_d being the density and average energy of deep traps and σ the width of the trap distribution.

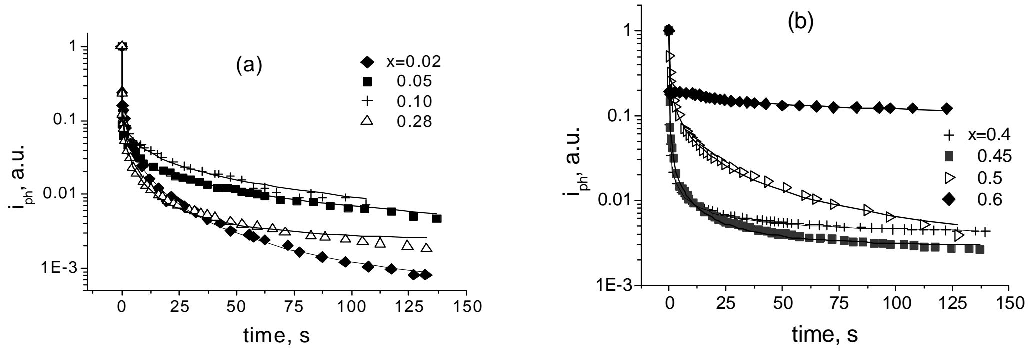

Fig. 1. The normalized photocurrent decay curves in As_xSe_{1-x} films at different As contents: (a) x<0.4, (b) x>0.4. The solid curves are the least-square fitting of photocurrent decay data by the stretched-exponential function.

For x=0.02 and x=0.5 these diagrams consist of a single broad maximum with σ about 0.035 eV. As the concentration of arsenic increase, the position of the peak shifts toward mid-gap from 0.69 to 0.73 eV. For other compositions (x=0.28, 0.4, 0.45 and 0.6) these diagrams are qualitatively different from those for lower x=0.02 and x=0.5.

Solid lines on figure represent an attempt to evaluate the original DOS distribution from experimental data by the use of equations (1), (2) and parameters: the peak energy E_d, the concentration N_t, width of deep trap distribution σ and characteristic Urbach energy E_0, listed in Table 1. Feature of the recovered DOS function is that, although the exponential band tail turns out to be reproduced reasonably well the maximum of the Gauss-form band of deep states gradually shifts to lower energies with increasing x>0.4.

In order to estimate the energy distribution of deep states the steady-state photocurrent spectra also were measured. Fig. 3 shows the photocurrent spectra for our samples. The broad maximum located at 1.8 eV corresponds to the band gap edge of As_2Se_3. Besides, we can observe a high sensitivity in the long-wavelength region of the spectrum due to existence of the deep states. In this region the photocurrent exponentially decrease with characteristic Urbach energy E_U. For x=0.02 this parameter take a value 0.079 eV. For x=0.05 and 0.1 the parameter E_U increase and take a values of about 0.1 eV. It seems, that chemical compositions essentially influences the parameters of the mid-gap states of amorphous As_xSe_{1-x} films.

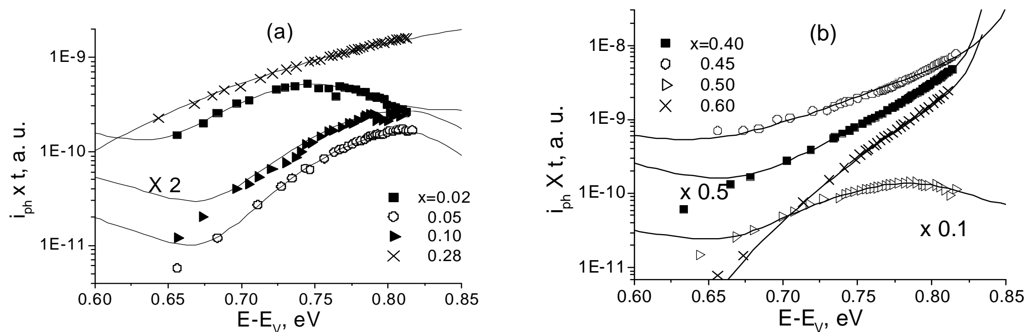

Fig. 2. i_{ph} (t) x t diagrams obtained with the help of curve in the Fig.1a and b for different As content: x < 0.4 (upper panel) and x > 0.4 (bottom panel). Solid lines represent model curves calculated on basis of Eq. (1) and (2).

Fig. 4 shows the photocurrent spectra for the non-stoichiometric As_xSe_{1-x} films as in Fig. 3 normalized to the spectra of the x=0.4 sample. This procedure allows us distinguish the additional absorption of the band gap states induced by chemical disordering. Only the photons that can be absorbed in As_xSe_{1-x} ($x \neq 0.4$) and can produce an excess of free carriers due to the localized states induced by new defects will cause an increase in photocurrent. As it seen from the Fig. 4, illumination with the sub-band gap light causes the features below the band edge around the 1.4 and 1.5 eV. The magnitude of the observed peak changes in dependence of chalcogenide film compositions. We suggest, that the intensity of absorbed light in this region is associated with the density of defects with negative U^-. Note, that the similar defect sub-band states have also been observed in AsSe films, and were attributed to A^+ level of the D^+ centers [14].

Table 1. The list of parameters for As_xSe_{1-x} amorphous films evaluated from PRT and steady-state photocurrent spectra.

x	τ, s	α	μ_c/R, $V^{-1}cm^{-1}$	N_d, cm^{-3}	E_d, eV	σ, eV	N_t, cm^{-3}	E_0, eV	E_U, eV
0.02	0.055	0.262	1.4e4	1.5e14	0.696	0.035	2.5e19	0.051	0.079
0.05	0.001	0.129	3.15e3	8.5e14	0.748	0.034	1.5e19	0.058	0.1
0.1	0.005	0.149	3e3	3.5e14	0.745	0.036	2e19	0.0546	0.11
0.28	0.011	0.220	1.1e5	8e17	0.76	0.086	1e19	0.08	0.07
0.4	0.001	0.144	2.4e5	2e17	0.84	0.07	8e19	0.065	0.064
0.45	0.0034	0.201	3.15e5	8.5e16	0.84	0.088	1.5e19	0.08	0.068
0.5	0.174	0.266	4e4	8e14	0.728	0.038	1e19	0.064	0.071
0.6	0.020	0.089	8.1e4	2e18	0.867	0.062	1e19	0.05	0.13

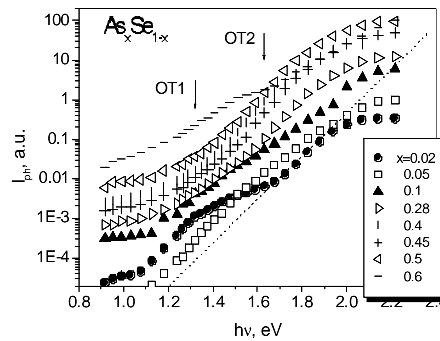

Fig. 3. Photocurrent spectra of As_xSe_{1-x} films measured at T=300 K for various As content x: 1 - 0.02, 2 - 0.05, 3 - 0.1, 4 - 0.28, 5 - 0.4, 6 - 0.45, 7 - 0.5, 8 - 0.6. For comparison the spectra are shifted along Y-axis by the factor: 2 - 3, 3 - 6, 4 -12, 5 - 24, 7 - 48, 8 - 96.

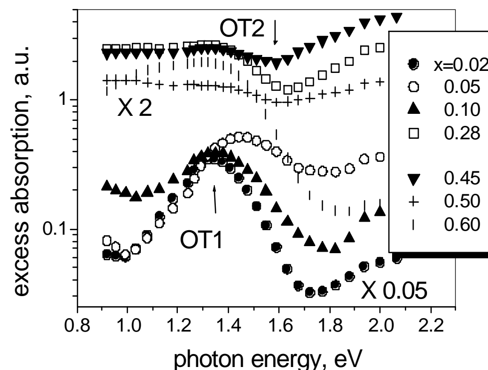

Fig. 4. Excess of the photocurrent spectra derived from the spectra as in Fig. 3 (see text for details).

5. Discussion

Our analysis of obtained data is based on comparison between x=0.02 and x=0.5 result. The i_{ph} x t diagrams of these films are essentially influenced by deep defects and have well-defined defect bump futures. We suggests that the diagram for x=0.02 associated with under-coordinated Se atoms because the peak is similar to that which occurs in a-Se and it occurs in the same energy range as in a-Se below mid-gap [9]. For high arsenic content the peak x=0.5 diagram is similar to that deduced from the optical absorption experiment and steady-state photocurrent spectra for As-Se layer [14]. Based on these arguments we may speculate that the deep states in the middle gap are due to over-coordinated Se atoms. For other compositions with high arsenic content the i_{ph} x t diagrams reveal a very broad DOS peak near 0.84 eV, close to Fermi level.

It is also evident, that the g(E) function evaluated from $i_{ph}(t)$ x t diagrams of amorphous As_xSe_{1-x} films each represent a broad Gauss-form band of deep states. With increasing x the positions of the maximum increase from 0.69 eV at x=0.02 to 0.89 eV at x=0.6. (see Table 1). For x=0.5 this defect band is considerably narrower than that in the samples with x=0.4. It is clear, the narrower the width of g(E)-distribution, the more ordered local structure. This suggests, that at high arsenic content (x>0.4) the film network dissociates into arsenic-rich smaller molecular clusters as was proposed in [7]. Such interpretations coincide with the rigid percolations approach: the more rigid film, the lowest concentration of U^- defect centers.

As it was established by Raman spectroscopy and nuclear quadruple resonance (NQR) measurements [15,16], for x<0.4 the amorphous network are locally flexible and exhibit strong electron-phonon interaction. This leads to formation of the D^+ and D^- defect centers with negative U^-. For x=0.4 the amorphous network becomes rigid and a small portion of this defects can be presented in film. However, for x>0.4 there exist other defects, related to As-As bonds whose densities increase with increasing x [7]. The interpretation is inferred from absorption spectra for analogous binary system As_xS_{1-x} (x=0.17-0.43), which were obtained using the photothermal deflection spectroscopy [17]. It was shown, that with increase in As content, the level of weak absorption tail (at a photon energy 1.5 eV) increases, which is consistent with our result. However, the absorption level becomes smaller in $As_{0.43}S_{0.57}$, it possible, due to As-As bonds that form extended states. In the As-rich films we expect that the bottom of the conduction band is mixed with the As-As anti-bonding state and slightly decreases. As result the DOS peak shifts to the lower energy for x>0.4 as shown in Fig. 2.

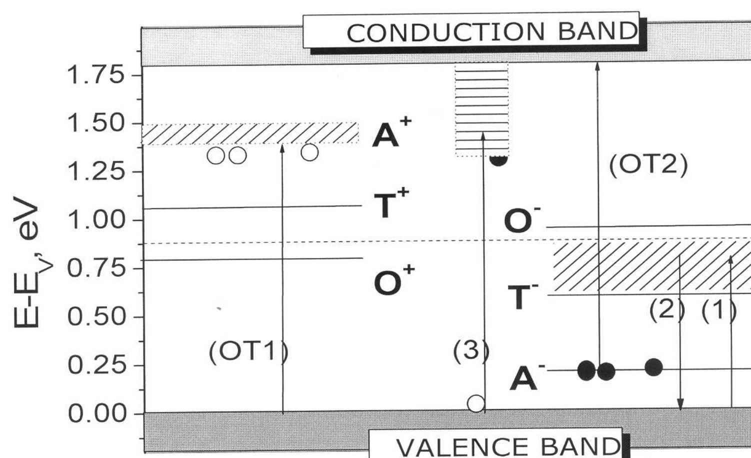

Fig. 5. The energy levels of D^+ and D^- defects with negative U^- for allowed thermal and optical (OT1, OT2) transitions in As-Se binary systems from [8]. The emission and capture processes determine the long term of photocurrent decay in our experiment.

In Fig. 5 we have presented the typical scheme of the energy levels for D^+ and D^- defects with negative effective correlation energy U^- upgraded with the quasi-continues band of deep states (the dashed rectangular) for allowed thermal transitions, that manifested in our experiment. The bottom of this band coincides with T^- level position for the thermal transitions in a-As_2Se_3, as referred in [8].

The Gauss peak of deep states also leads to a non-hyperbolic decay of the photocurrent, which is more pronounced at higher As content (persistent photocurrent). It is clear, that the deep states can be responsible for observed features in our measurements of photocurrent relaxations (as it occur in the long-term of photocurrent decay for x=0.6). The deeper trap, the greater time of the thermal emission for the localized carriers. Also the population of the deep trap near the Fermi level is sufficiently great and the deep capture is effectively suppressed.

6. Conclusions

We have studied the As_xSe_{1-x} amorphous films with x=0.02, 0.05, 0.1, 0.28, 0.4, 0.45, 0.5, 0.6 using PRT and steady-state photocurrent spectra at room temperature. The composition dependence of the long-wavelength component of photocurrent spectra is clear observed: with an increase in As content the level of this component increase. Also the long-term (persistent) photocurrent decay following the steady-state photoexcitation has been revealed. Comparisons with photocurrent spectra results shows, that variation of decay time with composition exhibits a change at the stoichiometric composition. It behavior can be interpreted in terms of the band-tails and deep acceptor-like centers presented in As_xSe_{1-x} films.

For the compositions with x=0.02 and x=0.5 the i_{ph} x t diagrams consist of a broad maximum, whose peak energy increase from 0.69 at x=0.02 to 0.88 at x=0.5. The diagrams for x=0.45 and x=0.5 are narrower. We have interpreted these results as arising from decrease deep states due to local ordering of the films. This explanation is supported by steady-state photocurrent spectra, from which the defect bump intensity at photon energies 1.4-1.5 eV also is decrease, in accordance with photocurrent spectra, known for stoichoimetric As_2Se_3.

References

[1] H. Fritzsche, Insulating and Semiconducting Glasses, ed. by P. Boolchand, World Scientific, Singapore, 2000, p. 653.
[2] K. Shimakawa, A. Kolobov, S. R. Elliott, Adv. Phys. **44**, 475 (1995).
[3] D. Lezal, J. Optoelectron. Adv. Mater **5**(1), 35 (2003).
[4] X. Zhang, H. Ma, J. Lucas, J. Optoelectron. Adv. Mater **5**(5), 1327 (2003).
[5] J. Teteris, M. Reinfelde, J. Optoelectron. Adv. Mater. **5**(5), 1355 (2003).
[6] M. Veinguer, A. Feigel, B. Sfez, M. Klebanov, V. Lyubin, J. Optoelectron. Adv. Mater. **5**(5), 1361 (2003).
[7] D. G. Georgiev, P. Boolchand, M. Micoulaut, Phys. Rev. B **62**, R9228 (2000).
[8] G. J. Adriaenssens, N. Qamhieh, N. Bollé, Electronic phenomena of chalcogenide glassy semiconductors, ed. by K.D. Tsendin, Science, Russian Academy of Sciences, St. Petersburg, 1996, p. 192 (in Russian).
[9] M. Kastner, D. Adler, H. Fritzsche, Phys. Rev. Lett. **37**, 1504 (1976).
[10] D. V. Harea, I. A. Vasilev, E. P. Colomeico, M. S. Iovu, J. Optoel. Adv. Mater. **5**, 1115 (2003).
[11] M. A. Iovu, M. S. Iovu, E. P. Colomeico, J. Optoelectron. Adv. Mater. **5**(5), 1209 (2003).
[12] M. S. Iovu, I. A. Vasiliev, E. P. Colomeiko, E. V. Emelianova, V. I. Arkhipov, G. J. Adriaenssens, J. Phys.: Condens. Matter **16**, 1 (2004).
[13] K. Shimakawa, Phys. Rev. B **34**, 8703 (1986).
[14] M. Iovu, S. Shutov, S. Rebeja, E. Colomeico, Phys. Stat. Sol. (b) **206**, 583 (1998).
[15] E. Ahn, G. A. Williams, P. C. Taylor, D. G. Georgiev, P. Boolchand, B. E. Schwickert, R. L. Cappelletty, J. Non-Cryst. Sol. **299-302**, 958 (2002).
[16] C. Derbidge, P. C. Taylor, J. Non-Cryst. Sol. **351**, 233 (2005).
[17] K. Tanaka, J. Optoelectron. Adv. Mater. **3**, 189 (2001).